THE RECURSIVE STACKING OPERATOR (RSO) PART 1: FROM RSO TO CRS PARAMETERS

B. Schwarz, C. Vanelle, and D. Gajewski

email: *benjamin.schwarz@zmaw.de*
keywords: *traveltimes, stacking, CRS, parameters*

ABSTRACT

The recursive stacking operator (RSO) is a double-square-root expression of the traveltime that depends on three unknown parameters and the overburden velocity. In the case of homogeneity above the reflector these quantities are intuitive and depth-related, however, they become effective parameters when velocity changes occur. We introduce two conceptually different transformations of the RSO parameters to the well-known and physically sound CRS attributes. While one attempt relies on the application of a time shift, the other one makes use of a Taylor series expansion of the squared RSO traveltime. For some special but very important acquisition and subsurface configurations both parameterizations reduce to familiar formulae. Numerical studies reveal that the approach based on a Taylor series expansion leads to higher accuracy than CRS and planar multifocusing over the full range of reflector curvatures for simple subsurface models.

INTRODUCTION

The common reflection surface (CRS) stack method (Müller, 1999) approximates the reflection response of an interface by a traveltime surface of second order, extending in offset and also midpoint direction. In the CMP gather, traveltime moveout is described by the classical NMO hyperbola, whose description is exact for the case of a planar dipping reflector beneath an overburden of constant velocity. Any deviation from this simple model causes the moveout to be nonhyperbolic (see, e.g. Fomel and Grechka, 2001).

One straight-forward attempt to better account for reflector curvature in the CMP gather is to assume the reflecting interface to be locally spherical. For this more general model, Vanelle et al. (2010) derived an implicit expression for the reflection traveltime by evaluating Snell's law. Since the expressions become explicit for the zero-offset case, this new operator is applicable in a recursive fashion. It is hence called 'recursive stacking operator' (RSO). RSO is parameterized in terms of three attributes and the overburden velocity, which represent real subsurface properties for the homogeneous case. Since, however, RSO was derived under the assumption of a homogeneous overburden, the parameters lose their physical meaning if heterogeneity is present. In this case, they can be considered effective parameters.

The well-known CRS parameters (Hubral, 1983) have a clear physical meaning and allow for very powerful applications (see, e.g. Duveneck, 2004). Therefore, it is important to relate these to the RSO parameters. In this work, we introduce two conceptually different parameterizations of the RSO expressions in terms of the CRS attributes. Due to the fact that only the functional form of the traveltime operator needs to be changed, the RSO can easily be integrated in any of the already existing CRS environments. Furthermore, we show that the two representations not only reduce to familiar formulae for some special subsurface and acquisition configurations, but that one of them provides noticeably higher accuracy than CRS as well as the double-square-root-based planar multifocusing (MF) expression (Gelchinsky et al.,

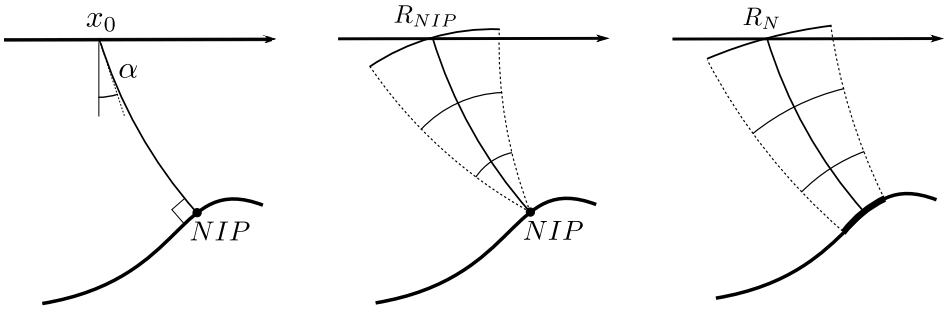

Figure 1: Illustration of the meaning of the CRS parameters: The quantities R_{NIP} and R_N are the radii of curvature of two so-called eigenwaves, the first stemming from a fictitious point source located at the normal incidence point (center), the latter resulting from an exploding reflector experiment around NIP (right). Both wavefronts emerge with the angle α (left) at the registration surface.

1999). This applies for the whole range of reflector curvatures and the gradient models considered in this work.

THEORY

Three kinematic wavefield attributes, i.e. α, R_{NIP} and R_N, were introduced by Hubral (1983) and can be appealingly interpreted in the framework of geometrical optics (see Figure 1). R_{NIP} and R_N are the radii of curvature of two so-called eigenwaves (Tygel et al., 1997). The NIP-wave stems from a fictitious point source placed at the point of normal incidence (NIP) on the reflector; the normal wave is the result of a fictitious exploding-reflector experiment in the vicinity of NIP. Both waves emerge with the angle α at the horizontal zero-offset position x_0 and contain distinct properties of the reflector, i.e. its distance, curvature and orientation, propagated to the registration surface.

Common reflection surface

A commonly used description of the traveltime is the CRS formula (Müller, 1999). In midpoint ($\Delta x_m = x_m - x_0$) and half-offset (h) coordinates, it reads:

$$t^2_{CRS}(\Delta x_m, h) = \left(t_0 + \frac{2\sin\alpha}{v_0}\Delta x_m\right)^2 + \frac{2t_0\cos^2\alpha}{v_0}\left(\frac{\Delta x_m^2}{R_N} + \frac{h^2}{R_{NIP}}\right) \quad , \tag{1}$$

where t_0 is the zero-offset traveltime and v_0 is the velocity at the surface.

Höcht et al. (1999) derived an implicit representation of the traveltime, which they refer to as parametric CRS. For the case of constant velocity over a spherical reflector, it represents the exact reflection response. Due to its implicit character, the parametric CRS is not implementable in an efficient way, since it requires trace interpolation. The CRS formula (1) is equivalent to a second-order Taylor series expansion of the parametric CRS, and hence an explicit expression.

Planar multifocusing

Gelchinsky et al. (1999) introduced a double-square-root expression for the traveltime, depending on the same set of parameters as the CRS method, namely the kinematic wavefield attributes α, R_{NIP} and R_N. Their operator describes the traveltime of a reflection event in terms of the traveltime of a central ray and

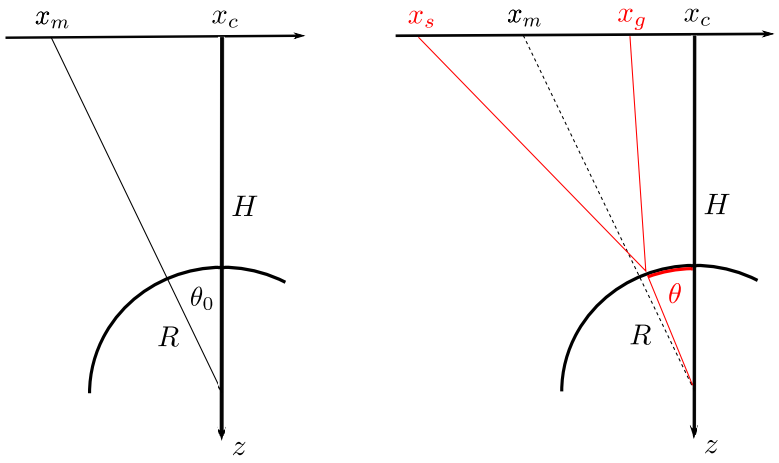

Figure 2: RSO evaluates the traveltime by finding the reflection point on a locally spherical interface, which is parameterized by the angle θ. For zero-offset, this quantity is an explicit expression. For nonvanishing offsets it is obtained recursively and the zero-offset angle θ_0 serves as a starting guess.

corrections applied at the source and receiver for a paraxial ray. It reads:

$$t_{MF}(\Delta x_s, \Delta x_g) = t_0 + \Delta t_s + \Delta t_g \quad , \tag{2a}$$

$$\Delta t_s = \frac{\sqrt{R_s^2 + 2R_s \Delta x_s \sin\alpha + \Delta x_s^2} - R_s}{v_0} \quad , \tag{2b}$$

$$\Delta t_g = \frac{\sqrt{R_g^2 + 2R_g \Delta x_g \sin\alpha + \Delta x_g^2} - R_g}{v_0} \quad , \tag{2c}$$

where

$$R_s = \frac{1+\sigma}{\frac{1}{R_N} + \frac{\sigma}{R_{NIP}}} \quad , \tag{3a}$$

$$R_g = \frac{1-\sigma}{\frac{1}{R_N} - \frac{\sigma}{R_{NIP}}} \tag{3b}$$

are the radii of two hypothetical waves focusing at the intersection of the central and paraxial ray. The quantities $\Delta x_s = x_s - x_0$ and $\Delta x_g = x_g - x_0$ are the horizontal displacements of source and receiver, respectively. The so-called focusing parameter σ can be designed to optimally fit the prestack data. Although spherical multifocusing expressions exist (see, e.g., Landa et al., 2010), in this work, we consider planar multifocusing only, where

$$\sigma(\Delta x_s, \Delta x_g) = \frac{\Delta x_s - \Delta x_g}{\Delta x_s + \Delta x_g + 2\frac{\Delta x_s \Delta x_g}{R_{NIP}} \sin\alpha} \quad . \tag{4}$$

Recursive stacking operator

The recursive stacking operator evaluates the reflection traveltime from a locally spherical interface by recursively updating the angle θ, which follows from an implicit expression (see Figure 2). For the homo-

geneous isotropic case it reads (Vanelle et al., 2010):

$$t_{RSO}(V, \delta x_c, H, R) = t_s + t_g \quad , \tag{5a}$$

$$t_s = \frac{1}{V}\sqrt{(\Delta x_m - h - \Delta x_c - R\sin\theta)^2 + (H - R\cos\theta)^2} \quad , \tag{5b}$$

$$t_g = \frac{1}{V}\sqrt{(\Delta x_m + h - \Delta x_c - R\sin\theta)^2 + (H - R\cos\theta)^2} \quad , \tag{5c}$$

$$\tan\theta = \tan\theta_0 + \frac{h}{H}\frac{t_s - t_g}{t_s + t_g} \quad , \tag{5d}$$

$$\tan\theta_0 = \frac{\Delta x_m - \Delta x_c}{H} \quad , \tag{5e}$$

where $\Delta x_c = x_c - x_0$. The quantity R represents the radius and $(x_c, 0, H)$ denotes the position of the middle point of the sphere approximating the reflector segment. Please note that $\Delta x_m - \Delta x_c = x_m - x_c$. For a homogeneous overburden these parameters are uniquely related to the subsurface geometry.

PARAMETERIZATION

The RSO parameters introduced in the previous section, namely Δx_c, H and R, only represent physical properties of the reflector segment if the velocity is constant. In the inhomogeneous case, they become effective (denoted by the tilde) parameters $\Delta\tilde{x_c}, \tilde{H}, \tilde{R}$ and cannot be related to the subsurface geometry anymore. In addition, the meaning of the quantity V is not clear, since it is assumed to be constant. As a consequence, V has to be treated as an effective parameter as well.

The CRS attributes can be interpreted as upwards propagated properties of the reflecting segment and therefore are surface-related. In consequence they have a clear physical meaning, regardless of velocity changes in the overburden.

In most existing stacking environments, the procedure is to sum all events along the best fitting operator and to place the result at (x_0, t_0). This means that a transformation not only has to incorporate α, R_{NIP} and R_N, but should also explicitly introduce t_0:

$$t(\tilde{V}, \Delta\tilde{x_c}, \tilde{H}, \tilde{R}) \quad \longrightarrow \quad t(t_0, \alpha, R_{NIP}, R_N) \quad . \tag{6}$$

Time shift

Even for inhomogeneous media, the wavefronts of the two eigenwaves can be approximated by circular arcs in the vicinity of the central midpoint location x_0 at the surface. In this case, the traveltime moveout can entirely be described in an auxiliary medium with the properties of the uppermost layer. Following Höcht et al. (1999) and de Bazelaire (1988), we can write:

$$\Delta t = \Delta t^I \quad . \tag{7}$$

Equation (7) simply states that the moveout Δt in the real subsurface model is equal to the moveout Δt^I in image space, i.e. the auxiliary medium with constant velocity v_0.

Since in a homogeneous medium the ray paths are straight, the RSO and CRS parameters are linked by geometry (see Figure 3):

$$\tilde{V}^s = v_0 \quad , \tag{8a}$$

$$\Delta\tilde{x_c}^s = -R_N \sin\alpha \quad , \tag{8b}$$

$$\tilde{H}^s = R_N \cos\alpha \quad , \tag{8c}$$

$$\tilde{R}^s = R_N - R_{NIP} \quad . \tag{8d}$$

The superscripts ^{s} in (8) indicate the time shift approach. Hence, (7) can be rewritten as:

$$\begin{aligned} t - t_0 &= t_{RSO}(\tilde{V}^s, \Delta\tilde{x_c}^s, \tilde{H}^s, \tilde{R}^s) - \frac{2R_{NIP}}{v_0} \\ \Leftrightarrow t &= t_{RSO}(\tilde{V}^s, \Delta\tilde{x_c}^s, \tilde{H}^s, \tilde{R}^s) - t_r \quad , \end{aligned} \tag{9}$$

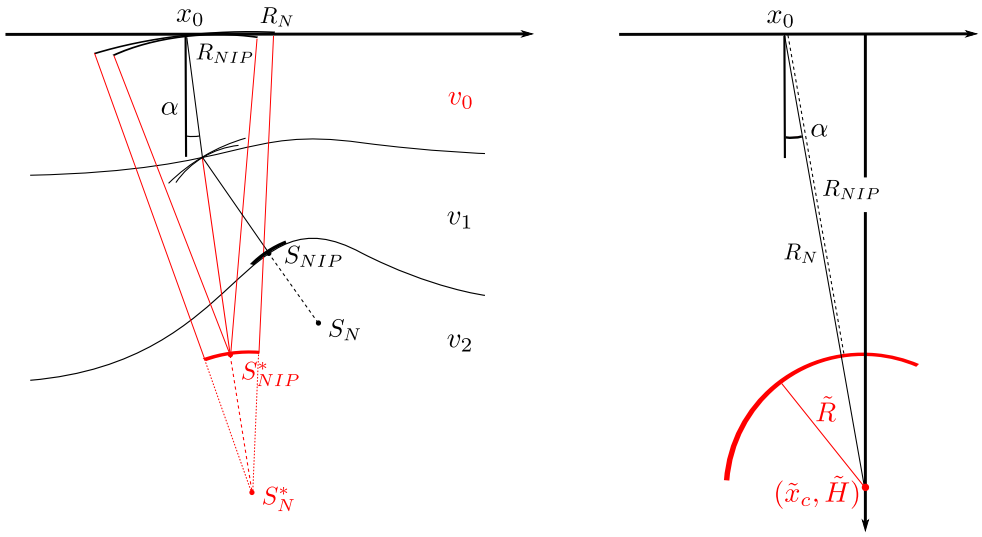

Figure 3: Illustration of the relationship between model and image space (left). Observed from x_0 at the registration surface, a ray originally initiated by a point source at S_{NIP} or an exploding reflector experiment around S_{NIP} with the center of local curvature at S_N seems to stem from a point source at S^*_{NIP} or an exploding reflector element with its center of curvature at S^*_N (after Höcht et al., 1999). Transformation of the RSO parameters $(\Delta\tilde{x_c}, \tilde{H}, \tilde{R})$ for the case of a constant velocity medium ($\tilde{V} = v_0$) is straight-forward, since the ray paths are straight (right).

with

$$t_r = \frac{2R_{NIP}}{v_0} - t_0 \tag{10}$$

and the RSO traveltime t_{RSO} defined according to (5).

For constant velocity overburden, (10) vanishes and the traveltimes in model and image space coincide. If the overburden is inhomogeneous, the RSO traveltime, with parameters transformed according to (8), is shifted by t_r.

A major advantage of this approach is that it not only follows physical intuition, but that it also explicitly introduces t_0. Since this parameterization of the recursive stacking operator incorporates the application of a time shift, it is from now on referred to as 'shifted RSO'. In mathematical context, the corresponding traveltime (9) is in consequence denoted t_{shift}.

Taylor series expansion

When expanding the square of the RSO traveltime (5), the coefficients up to second order have to be equal to the respective counterparts in the CRS formula.

To carry out the Taylor series expansion of the squared RSO traveltime (up to second order)

$$T(t^2_{RSO}) \approx c_0 + a_1\Delta x_m + b_1 h + a_2\Delta x_m^2 + b_2 h^2 \tag{11}$$

is rather tedious. To keep the focus on the new transformation formulae for the RSO parameters, only the resulting coefficients are presented here. Details can be found in Schwarz (2011).

With the abbreviations

$$\sin\tilde{\alpha} = \frac{\Delta\tilde{x_c}}{\sqrt{\Delta\tilde{x_c}^2 + \tilde{H}^2}} \quad , \tag{12a}$$

$$\tilde{R}_{NIP} = \sqrt{\Delta\tilde{x_c}^2 + \tilde{H}^2} - \tilde{R} \quad , \tag{12b}$$

$$\tilde{R}_N = \sqrt{\Delta\tilde{x_c}^2 + \tilde{H}^2} \tag{12c}$$

the combined zero-order term of the expansion c_0, reads:

$$c_0 = t_0^2 = \left(\frac{2\tilde{R}_{NIP}}{\tilde{V}} \right)^2 \quad . \tag{13}$$

Please note again at this point, that for the general case of inhomogeneity the straight-forward transformation

$$\begin{aligned} \tilde{V} &= v_0 \quad , \\ \tilde{R}_{NIP} &= R_{NIP} \end{aligned}$$

is not valid, since, as shown above, the zero-offset traveltime in image space generally differs from the actual one in model space. Only for homogeneous overburden these quantities are equal to each other and the time shift between image and model vanishes.

Coefficient b_1 describes the linear growth of the squared traveltime with offset. It vanishes:

$$b_1 = 0 \quad . \tag{14}$$

This result accords with our intuition and can be seen as a manifestation of the principle of reciprocity, which states that the traveltime of a ray originating at the source and arriving at the receiver position is the same as if the ray started at the receiver and traveled to the source.

The first-order coefficient describing the linear dependence of t_{RSO}^2 on the midpoint displacement Δx_m reads:

$$a_1 = \frac{4t_0 \sin\tilde{\alpha}}{\tilde{V}} \quad , \tag{15}$$

where t_0 is the square root of (13). The two remaining second-order coefficients a_2 and b_2 are:

$$a_2 = 2\frac{\tilde{V} t_0 \cos^2\tilde{\alpha} + 2\tilde{R}_N \sin^2\tilde{\alpha}}{\tilde{V}^2 \tilde{R}_N} \quad , \tag{16}$$

$$b_2 = \frac{2t_0 \cos^2\tilde{\alpha}}{\tilde{V}\tilde{R}_{NIP}} \quad . \tag{17}$$

As stated before, in order to fit into the CRS concept, c_0, a_1, a_2, b_1 and b_2 must be equal to their respective counterparts in the CRS traveltime formula (1). This leads to the following set of relations:

$$\frac{4t_0 \sin\tilde{\alpha}}{\tilde{V}} = \frac{4t_0 \sin\alpha}{v_0} \quad , \tag{18a}$$

$$\frac{2t_0 \cos^2\tilde{\alpha}}{\tilde{V}\tilde{R}_{NIP}} = \frac{2t_0 \cos^2\alpha}{v_0 R_{NIP}} \quad , \tag{18b}$$

$$\frac{2t_0 \cos^2\tilde{\alpha}}{\tilde{V}\tilde{R}_N} = \frac{2t_0 \cos^2\alpha}{v_0 R_N} \quad , \tag{18c}$$

$$\frac{2\tilde{R}_{NIP}}{\tilde{V}} = t_0 \quad . \tag{18d}$$

Since this system consists of four equations for four unknown parameters, namely $\tilde{V}$, $\Delta\tilde{x}_c$, $\tilde{H}$ and $\tilde{R}$, the

problem is well-determined and its solution provides the transformation of parameters:

$$\tilde{V}^t = \frac{v_{NMO}}{\sqrt{1 + \frac{v_{NMO}^2}{v_0^2}\sin^2\alpha}} \quad , \tag{19a}$$

$$\Delta\tilde{x}_c^t = \frac{-R_N \sin\alpha}{\cos^2\alpha\left(1 + \frac{v_{NMO}^2}{v_0^2}\sin^2\alpha\right)} \quad , \tag{19b}$$

$$\tilde{H}^t = \frac{v_0 R_N}{v_{NMO}\cos^2\alpha\left(1 + \frac{v_{NMO}^2}{v_0^2}\sin^2\alpha\right)} \quad , \tag{19c}$$

$$\tilde{R}^t = \frac{\frac{v_0 R_N}{v_{NMO}\cos^2\alpha} - \frac{v_{NMO}t_0}{2}}{\sqrt{1 + \frac{v_{NMO}^2}{v_0^2}\sin^2\alpha}} \quad , \tag{19d}$$

where the superscript ^{t} stands for Taylor series expansion and the normal moveout velocity is given by

$$v_{NMO} = \sqrt{\frac{2v_0 R_{NIP}}{t_0\cos^2\alpha}} \quad . \tag{20}$$

Since the equations (19) result from a Taylor series expansion of t_{RSO}^2, this parameterization will be referred to by the abbreviation 'Taylor RSO'. The corresponding traveltime expression reads:

$$t_{Taylor} = t_{RSO}(\tilde{V}^t, \Delta\tilde{x_c}^t, \tilde{H}^t, \tilde{R}^t) \quad , \tag{21}$$

where t_{RSO} is defined according to (5).

SPECIAL CASES

While in one parameterization a time shift is applied, the other one is based on a Taylor series expansion, which results in a pure double-square-root expression of the traveltime. Both not only provide the transformation from effective RSO parameters to the CRS attributes: they also incorporate the desired explicit introduction of the zero-offset traveltime t_0:

$$t_{shift} = t_0 + t_{RSO}(\alpha, R_{NIP}, R_N) - \frac{2R_{NIP}}{v_0} \quad , \tag{22}$$

$$t_{Taylor} = t_{RSO}(t_0, \alpha, R_{NIP}, R_N) \quad . \tag{23}$$

Hence they allow for a straight-forward implementation as a stacking operator.

To get more insight into the character of these two representations of the RSO traveltime, it is reasonable to investigate common acquisition and subsurface configurations. Details on the derivations can be found in Schwarz (2011).

Diffraction case

A diffractor, per definition, is an object of infinite curvature relative to the dominant seismic wavelength. In consequence, the number of wavefield attributes needed to properly approximate the corresponding response reduces to two since $R_N = R_{NIP}$. For shifted RSO as a result, $\tilde{R}^s$ according to (8) becomes equal to zero and the corresponding traveltime is entirely explicit:

$$\begin{aligned} t_{shift} - t_0 + \frac{2R_{NIP}}{v_0} = {} & \frac{1}{v_0}\sqrt{(\Delta x_m - h)^2 + 2(\Delta x_m - h)R_{NIP}\sin\alpha + R_{NIP}^2} \\ & + \frac{1}{v_0}\sqrt{(\Delta x_m + h)^2 + 2(\Delta x_m + h)R_{NIP}\sin\alpha + R_{NIP}^2} \quad . \end{aligned} \tag{24}$$

This expression also results from setting $R_N = R_{NIP}$ in the planar multifocusing operator (see (2)). For $\alpha = 0$, we obtain a time-shifted version of the double-square-root equation:

$$t_{shift} - t_0 + t_p = \sqrt{\frac{t_p^2}{4} + \frac{(\Delta x_m - h)^2}{v_0^2}} + \sqrt{\frac{t_p^2}{4} + \frac{(\Delta x_m + h)^2}{v_0^2}} \quad , \tag{25}$$

with $t_p = \frac{2R_{NIP}}{v_0}$.

For the case of varying velocity in the overburden and $R_N = R_{NIP}$ the Taylor RSO operator reduces to

$$t_{Taylor} = \sqrt{\frac{t_0^2}{4} + \frac{(\Delta x_m - h)^2}{v_{NMO}^2}} + \sqrt{\frac{t_0^2}{4} + \frac{(\Delta x_m + h)^2}{v_{NMO}^2}} \quad . \tag{26}$$

For horizontal layering, v_{NMO} can be substituted by the root-mean-square velocity v_{RMS}. In this case, (26) is equivalent to the Kirchhoff time migration operator. We observe that t_{Taylor} as well as t_{shift} becomes the exact diffraction response for the homogeneous case ($t_p = t_0$, $v_{NMO} = v_0$).

CMP gather, horizontal layering

While both parameterizations reduce to explicit expressions in the diffraction case, traveltime moveout in the CMP-gather, where $\Delta x_m = 0$, is in general described implicitly by the RSO approach (see (5)). However, when we assume horizontal layering in the subsurface ($\alpha = 0$, $R_N \to \infty$), the angle θ vanishes for both representations (see, e.g., Schwarz, 2011). For shifted RSO we get

$$\Leftrightarrow (t_{shift} - t_0 + t_p)^2 = t_p^2 + \frac{4h^2}{v_0^2} \quad , \tag{27}$$

with $t_p = \frac{2R_{NIP}}{v_0}$, which is equivalent to the shifted hyperbola (de Bazelaire, 1988). Again, shifted RSO provides the same description as the planar multifocusing operator (Landa, 2007). For the considered case of horizontal layering and restriction to the CMP-gather, Taylor RSO reduces to the classical NMO hyperbola:

$$t_{Taylor}^2 = t_0^2 + \frac{4h^2}{v_{NMO}^2} \quad . \tag{28}$$

Zero-offset section

In the zero-offset section the shifted RSO traveltime reads:

$$\left(t_{shift} - t_0 + \frac{2R_N}{v_0}\right)^2 = \frac{4}{v_0^2}\left[\Delta x_m^2 + 2\Delta x_m R_N \sin\alpha + R_N^2\right] \quad , \tag{29}$$

coinciding with the parametric CRS traveltime (Höcht et al., 1999), which is an explicit expression for the zero-offset case. In addition, it also coincides with the planar multifocusing traveltime expression, which Keydar et al. (1990) found to be equivalent to a hyperbola shifted in midpoint and time:

$$(t_{shift} - t_{apex} + t_p)^2 = t_p^2 + \frac{(x_m - x_{apex})^2}{v_0^2} \quad , \tag{30}$$

with

$$x_{apex} = x_0 - R_N \sin\alpha \quad , \tag{31a}$$

$$t_{apex} = t_0 + \frac{2R_N}{v_0}(\cos\alpha - 1) \quad , \tag{31b}$$

and

$$t_p = \frac{2\tilde{H}^s}{v_0} = \frac{2R_N}{v_0}\cos\alpha \quad .$$

Taylor RSO describes the zero-offset diffraction response by a midpoint-wise shifted hyperbola:

$$t_{Taylor}^2 = t_{apex}^2 + \frac{4(x_m - x_{apex})^2}{(\tilde{V}^t)^2} \quad , \tag{32}$$

with

$$x_{apex} = x_0 - \frac{v_0 t_0 R_{NIP} \sin\alpha}{v_0 t_0 \cos^2\alpha + 2R_{NIP}\sin^2\alpha} \quad , \tag{33a}$$

$$t^2_{apex} = \frac{t_0^3 v_0 \cos^2\alpha}{v_0 t_0 \cos^2\alpha + 2R_{NIP}\sin^2\alpha} \quad , \tag{33b}$$

and $\tilde{V}^t$ according to (19a). Expressions (33) perfectly coincide with the apex location Mann (2002) derived for the CRS traveltime formula for the diffraction case in the zero-offset section. We find that $t_{Taylor}(h = 0, R_N = R_{NIP})$ coincides with the Kirchhoff-type poststack time migration operator (Mann, 2002).

ACCURACY STUDIES

For constant velocity, the new recursive approach was already demonstrated to be more accurate than CRS and planar multifocusing over the full range of reflector curvatures (Vanelle et al., 2010). We now compute RMS traveltime errors of shifted RSO and Taylor RSO for different constant vertical velocity gradients in the overburden and compare them to the ones gained for the CRS formula (1) and the double-square-root-based planar multifocusing expression (2).

The basic geometry underlying all studies is a spherical reflector. The accuracy is evaluated for four different curvatures ranging from R =10 m, representing the limiting diffraction case to R =10000 m, i.e. a nearly planar interface. The vertical depth of the reflector, i.e. $H - R$, is kept constant at 1000 m. For all investigations we have a maximum offset of 2000 m, i.e. a maximum offset-over-depth-ratio of two. The horizontal midpoint displacements from the middle point of the circle range from -2000 m to 2000 m, i.e. are symmetric to $x_m = x_c$. To evaluate how inhomogeneity affects the accuracy for different curvatures four constant vertical velocity gradients are chosen:

$$v(z) = v_0 + \gamma z, \qquad \gamma = (0, 0.5, 1, 1.5)\frac{1}{s} \quad , \tag{34}$$

with v_0 =2 $\frac{km}{s}$. Although values of 1 $\frac{1}{s}$ and 1.5 $\frac{1}{s}$ for γ can be considered unrealistically strong, they help to judge the performance of each operator under extreme conditions.

Since we entirely deal with constant vertical velocity gradient media, analytical ray tracing is applicable and serves for the calculation of the reference traveltimes.

Influence of the number of iterations

The RSO traveltime description (5) is an inherently implicit expression since the angle θ, which needs to be known for the computation of t, itself depends on t_s and t_g. A possible way to overcome this problem is to compute the explicit zero-offset angle θ_0 to serve as a starting value and apply (5d) iteratively (see Vanelle et al., 2010). The recursive formula for n iterations reads:

$$\tan\theta_n = \tan\theta_0 + \frac{h}{\tilde{H}} \frac{t_s(\theta_{n-1}) - t_g(\theta_{n-1})}{t_s(\theta_{n-1}) + t_g(\theta_{n-1})} \quad , \tag{35}$$

where θ_n and θ_{n-1} are the values of θ gained after the application of n and $n-1$ iterations, respectively.

Figure 4 shows the RMS traveltime error distribution of shifted RSO and Taylor RSO for the four considered gradients after 0, 1, 10 and 100 iterations. We show only the R =10000 m case since here the effect of iterations becomes most noticeable. Please note that the general behavior is equivalent for smaller radii.

We observe that already a single iteration significantly increases the accuracy compared to the zero-iteration case, i.e. $\tan\theta = \tan\theta_0$, for weak gradients. For constant velocity, the accuracy of RSO can be increased by several orders of magnitude for 10 iterations and up to machine precision for 100 iterations, where double precision was used. Since, however, RSO already happens to be very accurate for one update of θ, even in this case one iteration occurs to be sufficient. For varying gradients, neither parameterization of the RSO approach shows increased accuracy for more than one iteration. In conclusion, all further results are gained by applying (35) only once.

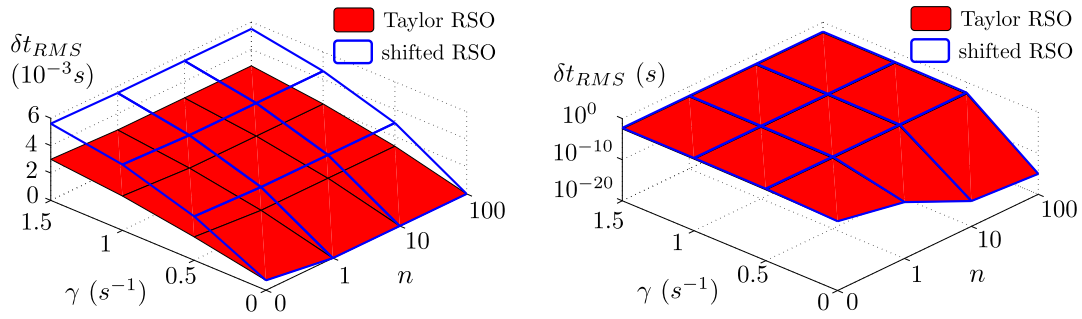

Figure 4: RMS traveltime error distributions for shifted RSO and Taylor RSO for R =10000 m as a function of γ and the number of iterations. One iteration provides a sufficient increase in accuracy, especially for the case of constant velocity in the overburden. For $\gamma > 0$ this effect becomes smaller and is overall barely noticeable. Please note the logarithmic scale on the right.

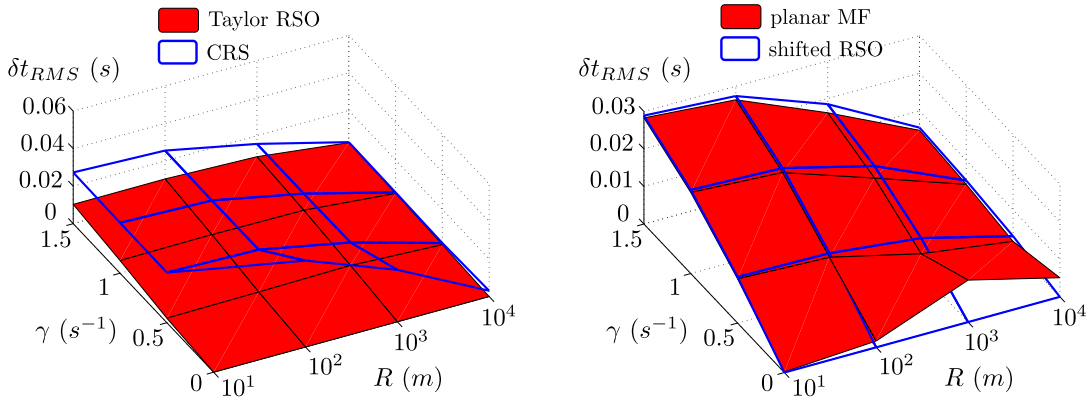

Figure 5: RMS traveltime error of the four considered operators as a function of curvature and gradient. The CRS description is only mildly affected by inhomogeneity in the overburden. Although the impact of velocity variation shows more noticeably for Taylor RSO, it still provides a significantly better fit than all other descriptions for all considered values of R. Shifted RSO and planar multifocusing perform equivalently over the full range of curvatures and all nonvanishing values of γ. Please note the different scales.

Comparison of RSO, CRS, and planar multifocusing

In Figure 5, the RMS traveltime errors of the four operators as a function of gradient and curvature are displayed. Although CRS overall presents itself as a little more stable in terms of velocity variation than the three double-square-root-based expressions, it still happens to be considerably less accurate for small radii. We observe that the new descriptions shifted RSO and Taylor RSO, as well as planar multifocusing are more accurate for values of R up to 1000 m for all tested gradients. Only for R =10000 m CRS is a little more accurate than planar MF and shifted RSO. The Taylor RSO operator shows higher accuracy than the others over the whole range of R and γ. Even for the case of R =10000 m, δt_{RMS} is slightly lower for Taylor RSO than for CRS (for all values of γ). A comparison of both RSO expressions reveals that the parameterization approach based on a Taylor series expansion handles inhomogeneity significantly better than the shifted approach. Moreover, shifted RSO and planar multifocusing show a resemblance in their RMS error distributions, thus confirming the preceding findings for the special acquisition and subsurface configurations. Only for the homogeneous case ($\gamma = 0\frac{1}{s}$) the error distributions differ noticeably. For all considered values of γ, CRS provides a considerably poorer fit than the double-square-root-based operators, if events stem from highly curved interfaces.

CONCLUSIONS AND OUTLOOK

We have introduced two different transformations from RSO to CRS parameters. While one of them is based on concepts of geometrical optics and incorporates the application of a time shift, the other is the result of a Taylor series expansion.

Both representations reduce to well-known formulae for specific acquisition and subsurface configurations. While the parameterization based on a Taylor series expansion and the hyperbolic CRS formula provide an equivalent description for horizontally layered media in the CMP configuration and of diffraction events in the zero-offset section, the time-shift-based representation coincides with planar multifocusing for all considered scenarios. Both versions of the RSO formula are exact for diffractions in a constant velocity medium.

Although based on the same underlying expressions, these two parameterizations of the RSO traveltime behave slightly differently in the presence of inhomogeneity. For the very simple case of a spherical reflector beneath a constant vertical velocity gradient overburden, the parameterization based on a Taylor series expansion provides higher accuracy for all considered curvatures and gradients. Besides the case of a homogeneous overburden, the time-shift-based version of RSO and planar multifocusing perform equally well. Furthermore, the numerical studies revealed that iterative application does not lead to an increase in accuracy if inhomogeneity is present. Already the first angle update provides high accuracy. Because of the nonhyperbolicity of diffraction events in offset direction, CRS is considerably less accurate for very high curvatures than the double-square-root-based descriptions.

In a subsequent study, Schwarz et al. (2011) show that the presented expressions not only provide more accurate traveltimes, but that they also lead to an improved stacked section and more reliable attribute estimates than CRS when applied to complex heterogeneous models. Since down- and upgoing ray segments are treated independently, the RSO traveltime formula allows for an extension to PS-converted waves and even anisotropy. Vanelle et al. (2011) have introduced a more general recursive formulation of the traveltime, which accounts for anisotropy in the overburden and provides the same high accuracy over the full range of reflector curvatures as shown in this work for the isotropic case. Future work includes the straight-forward extension of the presented concepts to 3D and application to field data.

ACKNOWLEDGEMENTS

We thank the members of the Applied Seismics Group Hamburg for continuous and fruitful discussions. We are grateful to Evgeny Landa from OPERA for providing the multifocusing software. This work was kindly supported by the sponsors of the Wave Inversion Technology Consortium. Seismic Un*x routines were used to compute reference traveltimes.

REFERENCES

de Bazelaire, E. (1988). Normal moveout revisited – inhomogeneous media and curved interfaces. *Geophysics*, 53:143–157.

Duveneck, E. (2004). Velocity model estimation with data-driven wavefront attributes. *Geophysics*, 69:265–274.

Fomel, S. and Grechka, V. (2001). Nonhyperbolic reflection moveout of P-waves: An overview and comparison of reasons. *Technical report CWP-372, Colorado School of Mines*. http://www.cwp.mines.edu/Meetings/Project01/cwp372.pdf.

Gelchinsky, B., Berkovitch, A., and Keydar, S. (1999). Multifocusing homeomorphic imaging – part 1. Basic concepts and formulae. *Journal of Applied Geophysics*, 42:229–242.

Höcht, G., de Bazelaire, E., Majer, P., and Hubral, P. (1999). Seismics and optics: hyperbolae and curvatures. *Geophysics*, 42:261–281.

Hubral, P. (1983). Computing true amplitude reflections in a laterally inhomogeneous earth. *Geophysics*, 48:1051–1062.

Keydar, S., Gelchinsky, B., Shtivelman, V., and Berkovitch, A. (1990). Common evolute element (CEE) stack and imaging (zero-offset stack). *SEG, Expanded Abstracts*, 9:1719–1722.

Landa, E. (2007). *Beyond conventional seismic imaging*. EAGE.

Landa, E., Keydar, S., and Moser, T. J. (2010). Multifocusing revisited – inhomogeneous media and curved interfaces. *Geophysical Prospecting*, 58:925–938.

Mann, J. (2002). *Extensions and Applications of the Common-Reflection-Surface Stack Method*. PhD thesis, Universität Karlsruhe.

Müller, T. (1999). *The Common Reflection Surface stack method – Seismic imaging without explicit knowledge of the velocity model*. PhD thesis, Universität Karlsruhe.

Schwarz, B. (2011). A new nonhyperbolic multi-parameter stacking operator. Master's thesis, Universität Hamburg.

Schwarz, B., Vanelle, C., and Gajewski, D. (2011). The recursive stacking operator (RSO) part 2: Application to heterogeneous media. *15th Annual WIT report*.

Tygel, M., Müller, T., Hubral, P., and Schleicher, J. (1997). Eigenwave based multiparameter traveltime expansions. *SEG Expanded Abstracts*, 16:1770–1773.

Vanelle, C., Bobsin, M., Schemmert, P., Kashtan, B., and Gajewski, D. (2011). RSO: a new multiparameter stacking operator for an/isotropic media. *15th Annual WIT report*.

Vanelle, C., Kashtan, B., Dell, S., and Gajewski, D. (2010). A new stacking operator for curved subsurface structures. *SEG, Expanded Abstracts*, 29:3609–3613.